Self-Replicating Holes in a Vertically Vibrated Dense Suspension

H. Ebata and M. Sano

Department of Physics, Graduate School of Science, The University of Tokyo, Tokyo 113-0033, Japan

(Received 12 April 2011; published 16 August 2011)

We find self-replicating holes on the surface of a vertically vibrated potato starch suspension. Above certain acceleration, the finite-amplitude deformation of the surface grows to form a hole that penetrates the fluid layer. The circular shape of the hole is not stable, and the hole begins to replicate just like the self-replicating spots in chemical reaction-diffusion systems. At high acceleration, these holes exhibit spatiotemporal chaos. By assessing the statistical properties in a steady state, we show that fluctuation in the number of holes can be understood by a master equation.

DOI: 10.1103/PhysRevLett.107.088301 PACS numbers: 47.57.−s, 47.20.−k, 47.52.+j, 47.54.−r

Various emergent patterns can be found in natural phenomena when systems are driven out of equilibrium. When the same pattern is found in completely different systems, it is natural to think of underlying laws which commonly govern the different systems. Self-replicating spots reminiscent of biological cell replication have been discovered in an experiment and a model of a chemical reaction-diffusion system [1,2]. The spots grow until they reach a critical size and then split into two. As the system is driven farther out of equilibrium, these spots replicate and annihilate persistently. Although features of self-replication in reaction-diffusion systems have been studied well theoretically [3,4], they have only been found in a chemical reaction system [1], and quantitative characterization is lacking. We report an observation of self-replicating holes in a fluid system. Instabilities of a vertically vibrated non-Newtonian fluid provide a prototype experimental system that is suitable for elucidating the replication or annihilation process and quantitative characteristics of weak turbulence in self-replicating systems.

There has been growing interest in instabilities and rheological properties of non-Newtonian fluids, including surface instabilities induced by vertical vibration [5,6]. Merkt *et al.* discovered persistent holes in a vertically vibrated cornstarch suspension or a glass microsphere suspension [7]; the holes persist despite the hydrodynamic pressure of the surrounding fluid. Ebata *et al.* found holes that expand rather than persist [8]. When a potato starch suspension was vertically vibrated, the deformation of the surface also grew to form a hole; however, the dynamics of these holes changes dramatically. Holes in potato starch suspension have a typical size of ∼5 mm, which is similar to that of a stable hole in a cornstarch suspension. However, the circular shape of the hole is unstable, and it begins to replicate similar to self-replicating spots in reaction-diffusion systems [see Figs. 1(a)–1(d)]. Above certain acceleration, the holes continuously replicate and annihilate as they spread out upon the surface of the suspension. It is known that self-replicating spots in a Gray-Scott model show spatiotemporal chaos (STC) in a certain parameter range [9,10]. We find that self-replicating holes also show spatiotemporal chaos at high acceleration (Fig. 1(e) and 1(f) [11]). In this Letter, we report detailed dynamics and statistics of self-replicating holes. A statistical analysis for defect-mediated turbulence [12,13] is applied to replicating holes. Statistical properties of birth and death rates of holes are similar to those in the Gray-Scott model [10], with minor nonlinear modifications despite considerable dissimilarity between surface instability and reaction-diffusion systems.

For the suspension, we used a mixture of potato starch (Sigma Aldrich) and water [14]. The powder was dried at 50 °C for one week and then stored in a desiccator. Before the experiment, a small amount of the powder (1 g) was baked at 105 °C for 2 h. From the decrease in weight, we

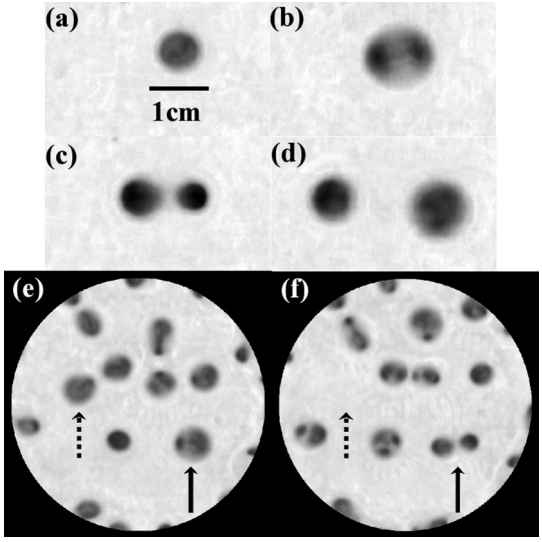

FIG. 1. (a)–(d) Time evolution of a self-replicating hole. A frame is taken every 1.6 s; (e),(f) spatiotemporal chaos of the holes (see video in [11]); Fig. 1(f) is the image taken 1.5 s after Fig. 1(e). Dashed arrows mark a hole annihilating by collision and solid arrows mark a hole replicating. The parameter values are $\phi = 0.47$, $f = 100$ Hz [(a)–(f)], and $\Gamma = 161$ m/s^2 [(a)–(d)], 180 m/s^2 [(e),(f)].

estimated the wetness of the powder (typically, wetness is 9–11 wt %). We varied the mass fraction of the system $\phi = M_p/(M_p + M_w)$ from 0.44 to 0.49, where M_p and M_w are the mass of the powder and water, respectively. A layer of suspension (initial depth = 4.5 mm) in a cylindrical glass container (inner diameter = 9 cm) was subjected to vertical sinusoidal vibration [vertical position $z(t) = A\sin(2\pi ft)$] using an electromagnetic vibration system. The frequency f was varied from 40 to 120 Hz, and the peak acceleration $\Gamma = A(2\pi f)^2$ was varied up to 245 m/s^2. The container was sealed to reduce evaporation. A local perturbation was created by making a small hole in the flat surface with a stick. Then, we recorded the dynamics of holes with a charge-coupled-device (CCD) camera at 30 frames/s. To eliminate the effect of the wall, we measured only the holes in the center region (7.4 cm in diameter) of the container. To count the number of holes, the images were binarized. The background was subtracted before conversion, and the threshold for binary image processing was chosen to minimize counting errors.

The surface instability of self-replicating holes shows subcritical bifurcation, necessitating an initial deformation of the surface. For all the parameters we examined, holes were not created spontaneously. Hence, new holes were created only by initial perturbation or self-replication of holes. For dispersed particles, we also used glass beads whose diameters were larger than 50 μm, but we observed only expanding holes [8]. The mean diameter of the potato starch was about 30 μm, and a stable hole was found in <20 μm dispersed particles [7,8].

The cascading process of self-replication is illustrated in Figs. 1(a)–1(d). The circular shape of a hole is unstable, and therefore, a circular hole first grows to an ellipsoid [Figs. 1(a) and 1(b)]. Then, a partition gradually appears inside the hole and the minor axis of the hole begins to shrink [Figs. 1(b) and 1(c)]. The suspension around the hole pours into the partition, and the hole is divided into two holes [Fig. 1(c)]. The two holes repel each other and separate, after which they begin to replicate again [Fig. 1(d)]. Figure 2(a) is the x-y-t plot of the replicating holes near the critical acceleration, showing the replication and annihilation of the holes. The hole diameter oscillates synchronously with the vibration (typically at 100 Hz) [7], and it also oscillates periodically with a slow cycle (typically 1.5–4 s). At the end of each slow cycle, the hole tends to replicate. However, holes sometimes fail to replicate; they do not replicate or they replicate but one of the new holes disappears quickly (typically, shorter than 0.5 s). As the acceleration increases, the oscillation period decreases and less holes fail to replicate. Therefore, the density of the holes increases at higher acceleration. The interaction between holes is repulsive if two holes are very close. However, the holes attract each other at a mid-distance. When two holes collide, several processes can be observed: After collision, the holes may separate [i.e., bounce;

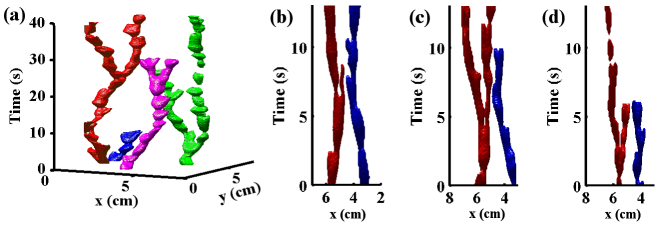

FIG. 2 (color online). Spatiotemporal plots of the binary images of the holes. Parameter values are $\phi = 0.47$, $f = 100$ Hz, and $\Gamma = 154$ m/s^2; (a) an x-y-t plot of the replicating holes; (b)–(d) collisions of the holes, with projections to the x-t plane; (b) bounce; (c) partial annihilation; and (d) pair annihilation.

Fig. 2(b)], one of the holes may annihilate [i.e., partial annihilation; Fig. 2(c)], or both holes may annihilate [i.e., pair annihilation; Fig. 2(d)]. Collided holes may also stick to each other for several seconds after they collide [see Fig. 2(c) from 5–10 s], but they do not merge. The dominant processes of annihilation are failure of replication and collision; isolated holes rarely annihilate spontaneously.

Figure 3(a) shows the phase diagram. Above the line in Fig. 3(a), holes continue to replicate and annihilate, and more than one hole always exists over 3 min. Below the line, holes may replicate for several seconds, but all holes cease to annihilate within 3 min. If the acceleration is sufficiently high, protrusion sometimes rises from the rim of the hole, as with the delocalized hole in [7]. When the acceleration is high enough, replication and annihilation of holes occur frequently, and eventually balance out. Therefore, the number of holes n fluctuates around a

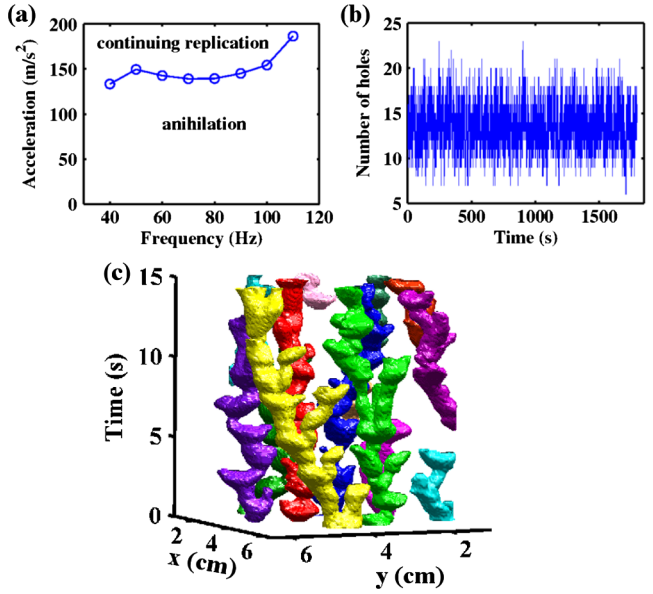

FIG. 3 (color online). (a) Phase diagram of replicating holes. Above the line, the holes continue to replicate for more than 3 min. (b) Fluctuation of number of holes in steady state; (c) an x-y-t plot of replicating holes in STC; parameter values are $\phi = 0.47$, $f = 100$ Hz, and $\Gamma = 180$ m/s^2 [(b),(c)].

mean value in the steady state. In Fig. 3(b), the mean value $\langle n \rangle = 13.2$ and standard deviation $\sigma = 2.25$ show strong fluctuations. Next, we calculated the spatial autocorrelation function and found that the correlation disappeared at the mean hole diameter. This indicates that hole positions are almost incoherent. The fluctuation in n and a short correlation length imply the existence of STC. The ratio of variance and mean value $\sigma^2/\langle n \rangle$ was introduced to measure the influence of spatial correlations [13]. In Fig. 3(b), the value of $\sigma^2/\langle n \rangle = 0.384$ of replicating holes is close to that of STC in the Gray-Scott model ($\sigma^2/\langle n \rangle = 0.448$, [10]). We also measured the power spectrum $S(f)$ of $n(t)$. For intermediate frequencies, we found a scaling of $S(f) \propto f^{-\kappa}$ with $\kappa \approx 1.8$–1.9 for various parameter values. This value is also close to that of STC in the Gray-Scott model ($\kappa \approx 2$, [10]). Figure 3(c) shows the x-y-t plot of the holes in STC. Comparing with Fig. 2(a), the dynamics of one hole does not change substantially; nonetheless, many replications, partial annihilations and pair annihilations can be seen. At low acceleration, the dominant process of the annihilation is failure of replication. However, at high acceleration, annihilation caused by collision often occurs as a result of attractive interaction and high density of holes. These frequent replications and annihilations cause STC.

The question is whether the replication and annihilation rates can be expressed by the total number of holes, i.e., whether the mean field picture can be applied to a self-replicating pattern. To elucidate it, we measured birth and death rates of the holes by image analysis and classified them [Fig. 4(a) inset, [15]). Birth events were classified as self-replication and inflow. Because we measured only near the center of the container, there was an inflow of holes from the outer regions of the container. Next, the death events were classified as annihilation (which includes failure of replication, spontaneous annihilation and annihilation by collisions) and outflow of holes to the outer region. By comparing the current image with the subsequent image over a short time interval (0.1 s), we counted the frequency of each event and then averaged the events over the time series ($\sim 18\,000$ frames). The replication rate does not increase proportionally to n but weakly [Fig. 4(a) inset]. So, as the hole density increases, the replication rate of one hole decreases. The annihilation rate is a quadratic function of n [Fig. 4(a) inset], which is in contrast to the linear function in the STC in the Gray-Scott model [10]. The quadratic term derives from collisions [12], but the annihilation rate also has a negative linear term and a positive constant term. The inflow rate is almost always larger than the outflow rate because of the wall effect [Fig. 4(a) inset].

Next, we calculated the birth rate by summing the replication and inflow rates. The death rate was calculated by adding the annihilation and outflow rates [Fig. 4(a)]. The birth rate $\Xi_+(n)$ was then fitted by a linear function and the death rate $\Xi_-(n)$ by a quadratic function [Fig. 4(a)]:

$$\Xi_+(n) = i_0 + i_1 n \tag{1}$$

$$\Xi_-(n) = d_0 + d_1 n + d_2 n^2. \tag{2}$$

In Fig. 4(a), these fitting parameters become $i_0 = 6.73$, $i_1 = -0.0248$, $d_0 = 3.07$, $d_1 = -0.786$, and $d_2 = 0.0768$. We examined the other parameters and found weak linear dependence of Ξ_+ on n and quadratic dependence of Ξ_- on n. Then, to determine the properties of the hole dynamics, we applied a probabilistic description as the extension of the model for defect-mediated turbulence [12]. Because of the short correlation length, a discrete birth-death Markov stochastic process with transition rates Ξ_+ and Ξ_- can be adopted [10].

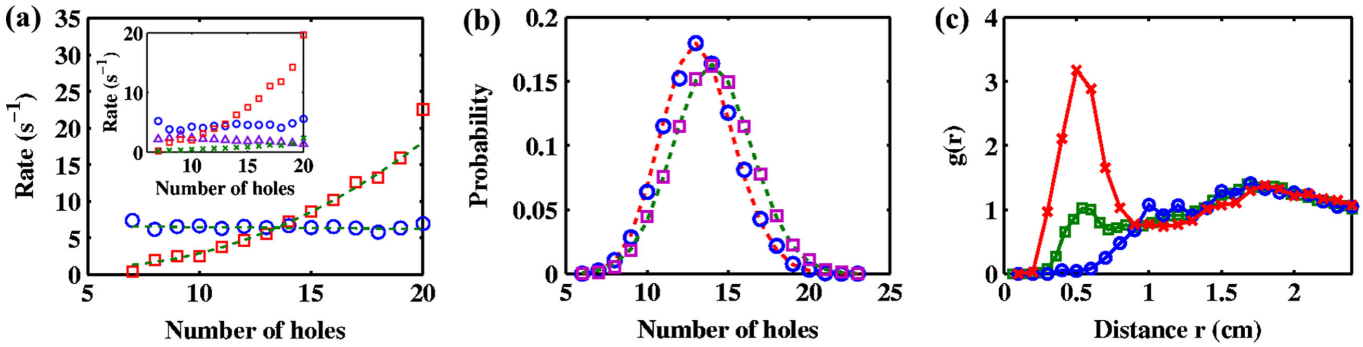

FIG. 4 (color online). (a) Birth (circle) and death (square) rate of holes as functions of the number of holes. Dashed curves are fitted using Eqs. (1) and (2). (Inset) Rate of each event; ○ replication, △ inflow, □ annihilation, × outflow. (b) Probability distribution function (PDF) of the number of holes. Circle and square symbols are calculated from time series of $n(t)$ [see Fig. 3(b)]. Dashed line is the PDF computed from Eq. (4). (c) Radial distribution function of the hole; square, circle, and cross are $g(r)$, $g_r(r)$, and $g_a(r)$, respectively. Parameters are $\phi = 0.47$, $f = 100$ Hz, and $\Gamma = 180$ m/s^2 [Figs. 4(a) and 4(c)]; $\phi = 0.47$, $f = 100$ Hz, and $\Gamma = 180$ m/s^2 [Fig. 4(b) ○]; and $\phi = 0.46$, $f = 80$ Hz, and $\Gamma = 180$ m/s^2 [Fig. 4(b) □].

$$P(n, t + dt) = P(n, t)\{1 - [\Xi_+(n) + \Xi_-(n)]dt\} + \Xi_+(n-1)P(n-1, t)dt + \Xi_-(n+1)P(n+1, t)dt \quad (3)$$

In the steady state, the master equation for the probability distribution function (PDF) of hole number $P(n)$ is reduced to $P(n) = \Xi_+(n-1)P(n-1)/\Xi_-(n)$. Based on Eqs. (1) and (2), a recursive relation leads to the following PDF:

$$P(n) = P(0) \prod_{j=0}^{j=n-1} \frac{i_0 + i_1 j}{d_0 + d_1(j+1) + d_2(j+1)^2}, \quad (4)$$

where $P(0)$ is the normalization factor.

Figure 4(b) illustrates the PDF $P(n)$ that is directly computed from the time series in Fig. 3(b). As shown in Fig. 4(b) (dashed line), the value of $P(n)$ calculated from Eq. (4) matches it quite well.

To investigate the spatial structures, a radial distribution function $g(r)$ was computed [Fig. 4(c)], where $g(r)$ is defined as $\langle \Omega(r) \rangle_t / (2\pi r dr \rho)$; ρ represents the average density of holes, and $\Omega(r)$ is the number of holes at distances from a given hole between r and $r + dr$. In addition, we selected $\Omega(r)$ whose centered hole is either annihilating or replicating. Next, we computed a radial distribution function around the annihilating holes $g_a(r)$ or replicating holes $g_r(r)$. $g(r)$ has a hard core region and the position of the first peak $r = 0.55$ cm corresponds to the mean diameter of the holes 0.54 cm. Thus, the first peak represents the situation in which two holes attach to each other. This indicates that the first peak reflects a replication of the hole. $g_a(r)$ also exhibit a very large peak at $\sim$0.5 cm. This indicates that most annihilating holes attach to other holes. Therefore, the first peak results from a failure of replication and collision. On the other hand, $g_r(r)$ has a larger hard core region and no sharp peaks. The larger hard core region clearly indicates that the hole cannot replicate if another hole approaches it. This supports the finding that the replication rate of one hole decreases as the total hole number increases [Fig. 4(a)]. These three radial distribution functions collapse when $r > 0.9$ cm. At this point, interaction length is estimated at 0.9 cm. Because of the interaction, the holes tend to form a loose linear structure, whose typical life span is $\sim$5 s. This spatial structure must affect the replication and annihilation rates. To fully understand the dynamics of the holes in STC, the interaction between holes will require further study.

Our results show that the statistical properties of self-replication are quite similar to the STC of reaction-diffusion systems despite the large dissimilarities between those and the fluid system presented here. This indicates that the self-replicating pattern might be one of the universal scenarios from localized pattern formation to weak turbulence. Another topic that remains to be addressed is the mechanism of the replicating hole. As stated in [7], these holes are only found in dense suspensions; therefore, the rheology of the dense suspension must deeply connect with the mechanism of holes. Recently, R. D. Deegan created a model of stable holes in which hysteresis in the shear rate response to applied stress was used [16]. We found that potato starch suspension also exhibits stress hysteresis. If the parameter values are carefully chosen, the metastable holes appear in the potato starch suspension. As the acceleration increases, these meta stable holes begin to replicate, suggesting that the rheological difference between the stable hole and replicating hole is not very large. While it is known that replicating patterns have hysteresis in local normal velocity to local curvature [4], it is not clear how a hole could have hysteresis in local normal velocity. To clarify the relationship between hysteresis in shear rate and that in local normal velocity, it will be necessary to calculate the influence of the hole shape on applied shear stress. Resolution of this issue should allow a more complete understanding of the important process of hole replication.

We thank E. Meron for valuable suggestions. This work is supported by JSPS.

[1] K-J. Lee *et al.*, Nature (London) **369**, 215 (1994).
[2] J. E. Pearson, Science **261**, 189 (1993).
[3] C. B. Muratov and V. V. Osipov, Phys. Rev. E **54**, 4860 (1996).
[4] C. Elphick, A. Hagberg, and E. Meron, Phys. Rev. E **51**, 3052 (1995).
[5] H. Shiba *et al.*, Phys. Rev. Lett. **98**, 044501 (2007).
[6] O. Lioubashevski *et al.*, Phys. Rev. Lett. **83**, 3190 (1999).
[7] F. S. Merkt *et al.*, Phys. Rev. Lett. **92**, 184501 (2004).
[8] H. Ebata, S. Tatsumi, and M. Sano, Phys. Rev. E **79**, 066308 (2009).
[9] Y. Nishiura and D. Ueyama, Physica D (Amsterdam) **150**, 137 (2001).
[10] H. Wang and Q. Ouyang, Phys. Rev. Lett. **99**, 214102 (2007).
[11] See Supplemental Material at http://link.aps.org/supplemental/10.1103/PhysRevLett.107.088301 for the videos of the replication of a hole and spatiotemporal chaos of the holes.
[12] L. Gil, J. Lega, and J. L. Meunier, Phys. Rev. A **41**, 1138 (1990).
[13] M. Hildebrand, M. Bar, and M. Eiswirth, Phys. Rev. Lett. **75**, 1503 (1995).
[14] As the solution, we also used a density matched aqueous solution of CsCl with density of 1.82 g/cm^3. In the density matched suspension, we also found a replicating hole.
[15] C.Beta *et al.*, Europhys. Lett. **75**, 868 (2006).
[16] Robert D. Deegan, Phys. Rev. E **81**, 036319 (2010).